Temperature Dependence of Resonance Raman Spectra of Metmyoglobin and Methemoglobin Azide. Detection of Resonance-Enhanced Bound Azide Vibrations and Iron–Azide Stretch†

Motonari Tsubaki, Raja B. Srivastava, and Nai-Teng Yu*

ABSTRACT: Resonance Raman spectroscopy has been employed to study the thermal spin equilibria in metmyoglobin azide [Fe(III)Mb·N_3] and methemoglobin azide [Fe(III)-Hb·N_3]. The effect of temperature on Raman intensities permits us to assign lines to either high- or low-spin species. With excitation at 647.1 nm the intensity of an $^{15}N_3$ isotope-sensitive mode at ~411 cm^{-1} was found to increase with decreasing temperature, indicating that its origin may not be the high-spin charge-transfer band at ~640 nm as suggested by Asher & Schuster [Asher, S. A., & Schuster, T. M. (1979) *Biochemistry 18*, 5377]. Instead, it may be enhanced via the weaker low-spin *z*-polarized charge-transfer band at ~650 nm which was identified by Eaton & Hochstrasser [Eaton, W. A., & Hochstrasser, R. M. (1968) *J. Chem. Phys. 49*, 985]. Our normal coordinate analysis on the model azide–Fe–imidazole and the polarized nature of the line allow us to establish that the ~411-cm^{-1} mode in Fe(III)Mb·N_3 and Fe(III)Hb·N_3 is assignable to the Fe–N_3 stretch of low-spin species. Furthermore, we assign the out of plane azide mode (low spin) to the depolarized line at 573 cm^{-1} ($^{15}N_3$ isotope sensitive), which was previously assigned as the Fe–N_3 stretch by Desbois et al. [Desbois, A., Lutz, M., & Banerjee, R. (1979) *Biochemistry 18*, 1510]. No internal vibrations of bound azide could be enhanced by excitation at 647.1 nm. However, upon excitation at 406.7 nm, we have observed the enhancement of the antisymmetric azide stretch (both high and low spin), out of plane bending (low spin), and Fe–N_3 stretch (low spin), indicating the existence of at least two charge-transfer transitions underlying the strong Soret band. The following four types of charge transfer are discussed in the light of our present resonance Raman data: (1) porphyrin (π) → high-spin Fe (d_π), (2) azide (n) → low-spin iron (d_{z^2}), (3) azide (π) → low-spin iron (d_{z^2}), and (4) azide (π) → porphyrin (π^*) (high spin).

Most ferric complexes remain in the same spin state over a wide temperature range, obeying the Curie–Weiss law. However, in some derivatives the energy separation between the high-spin ($S = {}^5/_2$) and low-spin ($S = {}^1/_2$) states is close to the thermal energy at room temperature so that they exhibit a temperature-dependent spin equilibrium. Thermal spin equilbria in metmyoglobin and methemoglobin derivatives such as azide, imidazole, hydroxide, and cyanate complexes have been extensively studied by magnetic susceptibility measurements (Beetlestone & George, 1964; Iizuka & Kotani, 1968, 1969a,b). If the low-spin state is the ground state, they obey the Curie–Weiss law in a low-temperature region where they are pure low spin. With increasing temperature their paramagnetic susceptibilities increase (reverse Curie law) and pass through a maximum in a transitional region, and finally the high- and low-spin states are equally populated according to their spin degeneracies, where they resemble the intermediate spin ($S = {}^3/_2$) state [for a review, see Iizuka & Yonetani (1970)].

Metmyoglobin– and methemoglobin–azide complexes have a low-spin ground state and exhibit a measureable spin equilibrium near room temperature (Iizuka & Kotani, 1968; 1969a,b). Equilibrium constants are different between myoglobin and hemoglobin derivatives and among different species. Such differences have been confirmed by infrared spectroscopy. McCoy & Caughey (1970) identified IR bands at 2023 and 2046 cm^{-1} in metmyoglobin azide [Fe(III)Mb·N_3] and at 2026 and 2048 cm^{-1} in methemoglobin azide [Fe(III)Hb·N_3] and have assigned them to antisymmetric stretch of bound azide. Their assignments of lower frequencies to low spin and higher frequencies to high spin were supported by Alben & Fager (1972) who showed that the relative intensities of the two IR bands exhibited a temperature dependence expected from a thermal spin equilibrium. The estimated equilibrium constant, i.e., $K^{25°C} = N_3(\text{low spin})/N_3(\text{high spin})$, was 18 for hemoglobin A, 8.1 for sperm whale myoglobin, and 7.0 for horse myoglobin.

Metmyoglobin azide (or methemoglobin azide) has an absorption band at ~640 nm, which has been assigned to an *x,y*-polarized high-spin charge-transfer transition (Eaton & Hochstrasser, 1968). When azide metmyoglobin is converted completely to the low-spin form (e.g., at 77 °C), the absorption spectrum still shows a weak broad band centered at ~650 nm, which was suggested by Eaton & Hochstrasser (1968) as a charge-transfer band (*z* polarized) corresponding to a transition of the *low-spin* form of metmyoglobin azide. By excitation into the 640-nm absorption region, Asher et al. (1977) observed the selective enhancement of a Raman mode at 413 cm^{-1} in methemoglobin azide and assigned it to the Fe(III)–azide stretch (without $^{15}N_3$ isotope evidence). Later, Desbois et al. (1979) assigned a 570-cm^{-1} mode (excited near Soret band) in metmyoglobin azide to the Fe(III)–azide stretch on the basis of a 16 cm^{-1} $^{15}N_3$ isotope shift. To explain the discrepancy between these two assignments, Asher & Schuster (1979) recently suggested that the 413-cm^{-1} mode was from high-spin and the 570-cm^{-1} mode from the low-spin form.

In this paper we demonstrate that with decreasing temperature the intensity of the 413-cm^{-1} mode increases in spite of the decrease in high-spin component (hence the absorption at ~640 nm). This is taken as a clear evidence that the 413-cm^{-1} mode derives its intensity from a weak *low-spin* charge-transfer band underlying the stronger *high-spin* charge

† From the School of Chemistry, Georgia Institute of Technology, Atlanta, Georgia 30332. *Received June 4, 1980.* N.-T.Y. is the recipient of National Institutes of Health Research Career Development Award (EY00073). The research activity in biophysical applications of Raman spectroscopy has been supported by grants (GM 18894 and EY 01746) from the U.S. National Institutes of Health.

0006-2960/81/0420-0946$01.00/0

transfer band at ~640 nm. Our temperature studies, isotope substitution, depolarization measurements, and normal coordinate analysis allow us to establish that the 413 and 570-cm^{-1} modes are Fe(III)–azide stretch and azide internal bending, respectively, both in low-spin state. In addition, we show the enhancement of bound azide antisymmetric stretch from both high- and low-spin forms upon excitation at 406.7 nm, indicating that charge-transfer transitions underlie the Soret absorption band.

Materials and Methods

Sperm whale myoglobin was obtained from Sigma Chemical Co. The lyophilized powder was dissolved in 0.01 M sodium phosphate buffer at pH 6.9 ($NaH_2PO_4 \cdot 2H_2O$, 2.26 g; Na_2HPO_4, 2.52 g/5 L) and was gel-filtered against the same buffer. The metmyoglobin solution was then applied to a column of CM-52 cellulose (Whatman) equilibrated with the same buffer. After being washed by ~500 mL of the buffer, the adsorbed metmyoglobin main component was slowly eluted by 0.025 M sodium phosphate buffer pH 7.2 ($NaH_2PO_4 \cdot H_2O$, 1.000 g; Na_2HPO_4, 1.325 g/L).

Human hemoglobin A solution was prepared in oxy form by usual procedures from whole blood (Kilmartin et al., 1975). Methemoglobin A was prepared by oxidation of oxyhemoglobin A with a slight excess of potassium ferricyanide, followed by extensive dialysis against 0.05 M sodium phosphate buffer, pH 7.2, ($NaH_2PO_4 \cdot H_2O$, 2.00 g; Na_2HPO_4, 2.65 g/L), and finally gel-filtered against the same buffer. The heme concentration was then determined spectrophotometrically in cyanide form by using the extinction coefficients of 10.7 and 11.0 mM^{-1} cm^{-1} at 540 nm for metmyoglobin cyanide and methemoglobin cyanide, respectively.

Azide and imidazole (Im) complexes of metmyoglobin and methemoglobin were formed by adding solid crystals directly into solution, and the pH value was checked, but there was usually no need to readjust. Imidazole (99% purity) was obtained from Aldrich and was further purified by recrystallization from benzene–chloroform. Triply labeled $Na^{15}N_3$ (99 atom %) and terminally labeled $K^{14}N^{14}N^{15}N$ (99.4 atom %) were purchased from Stohler Isotope Chemicals and Prochem, respectively.

Before Raman experiments, each sample solution was passed through a Millipore filter (pore size, 0.45 μm). The Raman cell (quartz) was kept in a rotating cell holder for laser irradiation to avoid local heating, and a 90° scattering geometry was used to obtain Raman spectra. Laser wavelengths at 406.7, 647.1, and 676.4 nm were provided by a Spectra-physics model 171-01 krypton ion laser and at 457.9 nm by CR-8 argon ion laser. Raman spectra excited at 406.7 and 457.9 nm were obtained by using a cooled SIT-detected multichannel Raman system (Yu & Srivastava, 1980). The detector (a dry ice cooled silicon-intensified target) is controlled by a Princeton Applied Research 1216 detector controller which provides power supply, scanning voltages, and processes signals for transmission to a microprocessor-based OMA 2 console (PAR 1215). The console provides keyboard control of all scanning functions. In addition, the console executed data acquisition, manipulation, and storage. The spectrometer used is a Spex 1402 0.85 m Czerny-Turner double monochromator which was modified to optimize resolution and spectral band-pass. The spectra obtained at each "window" were calibrated by using fenchone and CN^- by a special cubic fitting function in the OMA 2 console.

Because of slight fluorescence from samples and decrease in sensitivity of the cooled SIT detector in the red region, a conventional Raman system (Spex 1401 double monochromator and photon-counting electronics) was used for excitation at 647.1 and 676.4 nm. Raman frequencies obtained by mechanical scanning were calibrated by using fenchone and toluene. All the wavenumbers reported here are accurate within ±2 cm^{-1}.

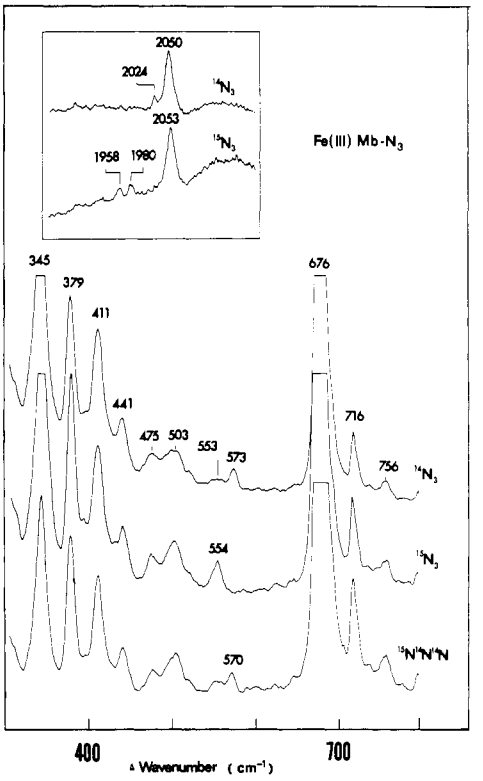

FIGURE 1: Resonance Raman spectra of Fe(III)Mb·$^{14}N_3$, Fe(III)-Mb·$^{15}N_3$, and Fe(III)Mb·$^{15}N^{14}N^{14}N$ in the 300–800-cm^{-1} and 1900–2100-cm^{-1} (inset) regions. Conditions: excitation wavelength (λ), 406.7 nm; laser power (p), 20 mW at sample; slit width (σ), 100 μm; data integration time (t), 30.3 s (1000 delay cycles, 10 readout scans); protein concentration, 0.033 mM; ligand concentration, ~1.0 mM; in 0.05 M sodium phosphate pH 7.2 buffer.

To avoid sample freezing in subzero temperature region, we used a 40% (v/v) glycerol buffer–water mixture as a solvent, which allowed us to decrease the temperature to −30 °C without freezing. The samples were kept at low temperature by a flow of cold N_2 gas through a Dewar enclosing the Raman rotating cell. By regulation of the cold nitrogen gas flow, the temperature could be maintained within ±1 °C. The temperature was measured by a copper–constantan thermocouple placed near the sample in the Dewar.

Results

The effects of $^{15}N_3$ and $^{15}N^{14}N^{14}N$ isotope substitution on the Raman spectrum of Fe(III)Mb·N_3 upon Soret excitation (λ = 406.7 nm) are shown in Figure 1. Three isotope-sensitive lines at 573, 2024, and ~2046 cm^{-1} were shifted to 554, 1958, and 1980 cm^{-1}, respectively. The ~2046-cm^{-1} line is hidden under a strong combination mode at 2053 cm^{-1} (i.e., 676 plus 1377 cm^{-1}) which was reported to be resonance enhanced upon Soret excitation (Champion et al., 1978). The 2024 and ~2046-cm^{-1} modes obviously correspond to the two infrared bands at 2023 and 2046 cm^{-1} which have been assigned (McCoy & Caughey, 1970; Alben & Fager, 1972) to bound azide antisymmetric stretch in low- and high-spin states, respectively. The 573-cm^{-1} line displays a 19-cm^{-1} shift upon substitution by $^{15}N_3$ and a 3-cm^{-1} shift by $^{15}N^{14}N^{14}N$. Desbois et al. (1979) assigned this mode to Fe(III)–N_3 stretch on the basis of the observed isotope shift. However, our depolarization

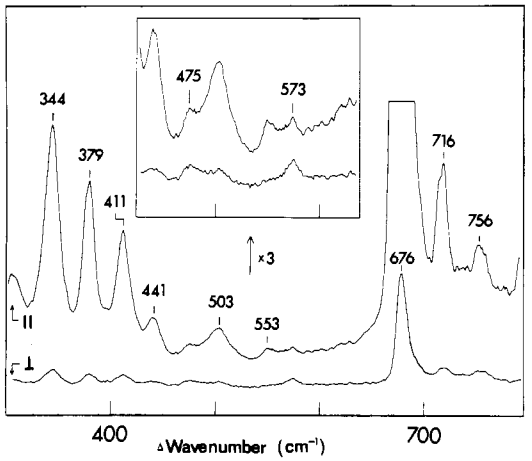

FIGURE 2: Parallel and perpendicular components of the resonance Raman spectrum of Fe(III)Mb·N_3 in the 300–800-cm^{-1} region, excited at 406.7 nm. In the inset the ordinate is enlarged 3 times. Note two depolarized modes at 475 and 573 cm^{-1}; the latter is assigned to internal azide bending (out of plane). Conditions: p, 25 mW at sample; σ, 200 μm; t, 303 s (10000 delay cycles, 100 readout scans); other conditions same as in Figure 1.

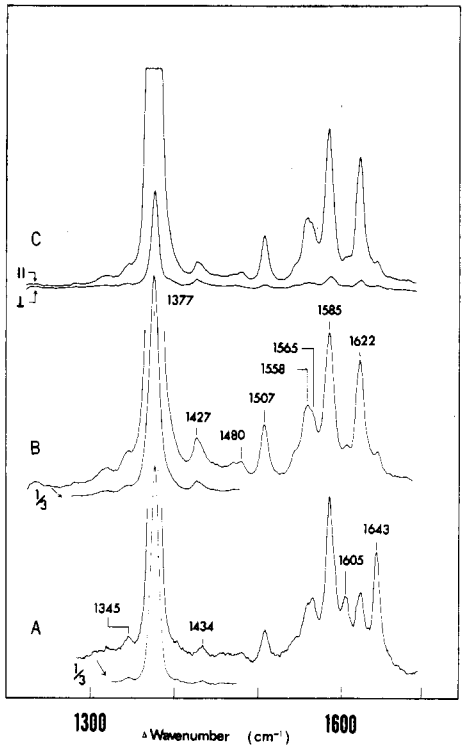

FIGURE 3: Higher frequency (1300–1700-cm^{-1}) resonance Raman spectra of Fe(III)Mb·N_3. (A) Spectrum excited at 457.9 nm. Conditions: p, 170 mW at sample; σ, 100 μm; t, 30.3 s; protein concentration, 0.025 mM; ligand concentration, ~5 mM; in 0.05 M sodium phosphate pH 7.2 buffer. (B) Spectrum excited at 406.7 nm. Conditions: p, 35 mW at sample; protein concentration, 0.033 mM; other conditions same as (A). (C) Parallel and perpendicular components of the resonance Raman spectrum excited at 406.7 nm. Conditions: same as in (B) except t = 303 s.

measurements indicate that this mode is *depolarized* (*dp*) (Figure 2), inconsistent with their assignment. A normal mode which is predominantly Fe(III)–N_3 stretch is expected to be *polarized* (*p*). As will become clear later, this 573-cm^{-1} mode is assignable to bound azide bending vibration when ferric iron is low spin. The assignment of the 573-cm^{-1} mode to low-spin species is consistent with the observation that this line decreases its intensity in carp methemoglobin azide when inositol hexaphosphate (IHP) is added to favor the high-spin component

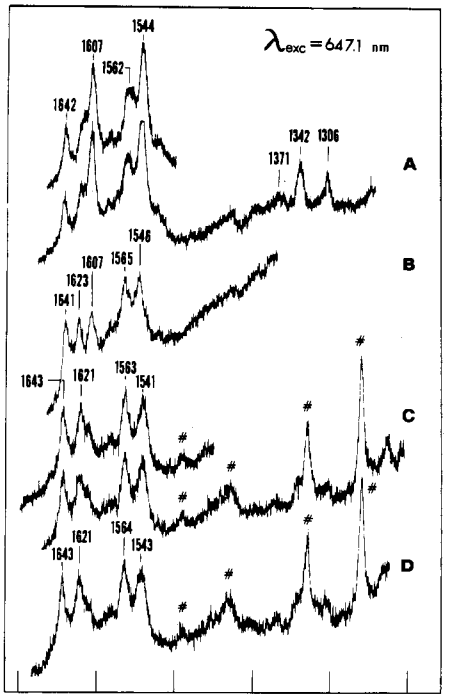

FIGURE 4: Higher frequency (1200–1700-cm^{-1}) resonance Raman spectra of Fe(III)Mb·N_3 (A), Fe(III)Hb·N_3 (B), Fe(III)Mb·Im (C), and Fe(III)Hb·Im (D) upon excitation at 647.1 nm. Conditions: p, 450 mW at sample; σ, 400 μm; time constant (τ), 5 s; scan speed (s), 0.2 cm^{-1}/s; protein concentration (heme basis), 1.1 mM for Fe(III)Mb, 1.2 mM for Fe(III)Hb; ligand concentration, azide ~20 mM, imidazole ~300 mM; in 0.05 M sodium phosphate buffer, pH 7.2. The mark (#) indicates lines from free imidazole.

(M. Tsubaki and N.-T. Yu, unpublished experiments; Debois et al., 1980). Recently, Yu & Tsubaki (1980) reported a depolarized (hence nontotally symmetric) bound azide bending mode at 650 cm^{-1} in the high-spin manganese(III)-substituted myoglobin–azide complex [Mn(III)Mb·N_3]. They also observed resonance enhancement of the bound azide antisymmetric stretch at 2039 cm^{-1} in the same complex, which has been explained in terms of vibronic couplings between azide (π) → porphyrin (π^*) charge-transfer state and nearby excited electronic states. It is therefore inferred that the enhancement of nontotally symmetric vibrations at 573 (azide bending), 2023, and 2046 cm^{-1} (azide antisymmetric stretch) requires similar vibronic couplings between a charge-transfer state (to be discussed later) and the Soret excited state.

In Figure 3 we present the spectra of Fe(III)Mb·N_3 in the 1300–1700-cm^{-1} region upon excitation near the Soret band (λ = 457.9 nm) (A) and at the Soret band (λ = 406.7 nm) (B and C). With excitation near the Soret band both low-spin (1643-cm^{-1}) and high-spin (1605-cm^{-1}) depolarized modes are clearly seen (Figure 3A). The polarized "spin-state indicators" at 1507 cm^{-1} (low spin) and 1480 cm^{-1} (high spin) (Spiro & Strekas, 1974) are also observable. The spectrum resembles the one excited at 488.0 nm, as reported by Kitagawa et al. (1976). By the excitation wavelength being tuned into the Soret band, the depolarized spin-state indicators at 1605 and 1643 cm^{-1} become very weak relative to the polarized ring modes. Again, the mode at 1507 cm^{-1} relative to the one at 1480 cm^{-1} indicates the dominance of the low-spin state in the spectra.

The spectral features in the 1300–1700-cm^{-1} region upon excitation at 647.1 nm (Figure 4) are quite different from those excited near or at the Soret band. Two high-spin lines at 1607 and 1544 cm^{-1} are the dominant features in the spectrum of Fe(III)Mb·N_3 (Figure 4A). The depolarized low-spin indi-

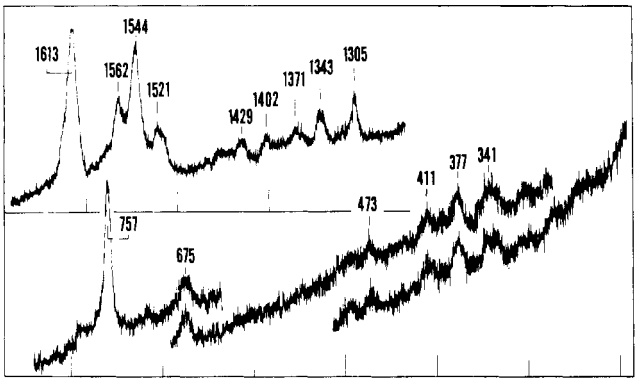

FIGURE 5: Resonance Raman spectra of Fe(III)Mb·H_2O in higher frequency (1300–1700-cm^{-1}) region (upper) and lower frequency (200–800-cm^{-1}) region (lower) with excitation at 647.1 nm. Conditions: σ, 450 μm; τ, 2.5 s; other conditions same as in Figure 4.

cator at 1642 cm^{-1} is somewhat weaker. The most dramatic change from violet to red excitation is the intensity reduction of the polarized mode at 1377 cm^{-1}. The weak line at 1371 cm^{-1} in Figure 4A may have a different origin from that at 1377 cm^{-1} in Figure 3.

The weak absorption bands around ~640 nm in Fe(III)-Mb·N_3, Fe(III)Hb·N_3, Fe(III)Mb·Im, and Fe(III)Hb·Im have been thought to be due to the presence of the high-spin species at room temperature (Beetlestone & George, 1964), because of (1) the analogy of the 640-nm band location to band I [according to the notation of Eaton & Hochstrasser (1968)] in the high-spin ferric hemoproteins, (2) the intensity of the 640-nm band in good correlation with the population of high-spin state at room temperature, and (3) the decrease of the 640-nm band intensity by decreasing the temperature, consistent with thermal spin transition from the high- to low-spin state (Eaton & Hochstrasser, 1968). Excitation within this absorption band gives rise to different intensity ratios between high-spin and low-spin indicators among various myoglobin and hemoglobin derivatives. The ratio of high-spin modes at 1607 and 1544 cm^{-1} relative to the low-spin mode at 1642 cm^{-1} is the largest for Fe(III)Mb·N_3 (Figure 4A) and smallest for Fe(III)Hb·Im (figure 4D). The Raman intensity ratio in decreasing order, Fe(III)Mb·N_3 > Fe(III)Hb·N_3 > Fe(III)Mb·Im > Fe(III)Hb·Im, correlates well with the absorption intensity around 640 nm or the percentage of high-spin species as measured by magnetic susceptibility, both at room temperature (Iizuka & Kotani, 1968, 1969a,b).

The Raman spectrum of aquo (acid) metmyoglobin [Fe(III)Mb·H_2O] with excitation at 647.1 nm [within band I, similar to the 640-nm band in Fe(III)Mb·N_3] is shown in Figure 5. Two depolarized "high-spin" lines at 1613 and 1544 cm^{-1} are strongly enhanced, and there is no line at ~1643 cm^{-1} from the low-spin state (Figure 5, upper spectrum). Except for disappearance of the 1643-cm^{-1} line the spectra of Fe(III)Mb·H_2O and Fe(III)Mb·N_3 in the 1300–1700-cm^{-1} region are very similar. The slight difference in dp mode frequency (i.e., 1613 vs. 1607 cm^{-1}) implies that the porphinato core (C_t–N distance) is smaller in high-spin Fe(III)Mb·H_2O than in high-spin Fe(III)Mb·N_3 (Spaulding et al., 1975; Spiro et al., 1979). These observations are consistent with the high-spin state origin of the 640-nm absorption band.

In Figure 6 we show the Raman spectra in the lower frequency region (250–800 cm^{-1}) of Fe(III)Mb·$^{14}N_3$ (A), Fe(III)Mb·$^{15}N_3$ (B), and Fe(III)Hb·$^{14}N_3$ (C) with excitation at 647.1 nm. The line at 411 [Fe(III)Mb·N_3] or 414 cm^{-1} [Fe(III)Hb·N_3] presumably corresponds to the 413-cm^{-1} mode reported by Ahser et al. (1977) in the spectrum of Fe(III)-

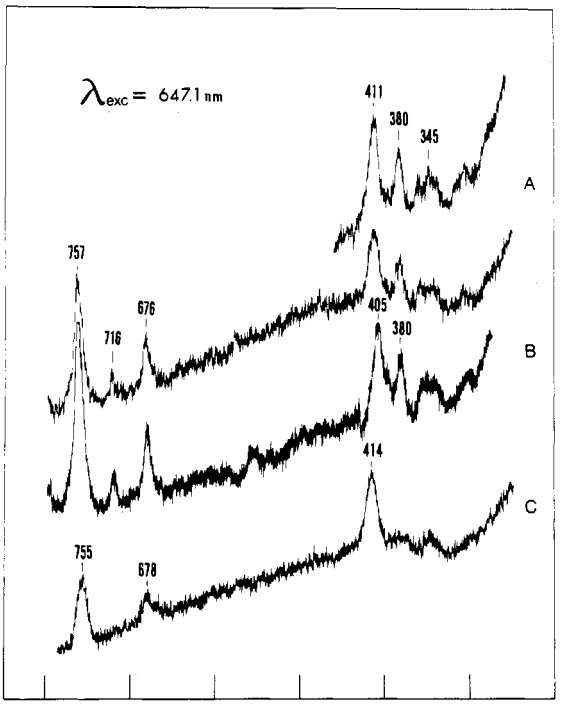

FIGURE 6: Lower frequency (200–800-cm^{-1}) resonance Raman spectra of Fe(III)Mb·$^{14}N_3$ (A), Fe(III)Mb·$^{15}N_3$ (B), and Fe(III)Hb·$^{14}N_3$ (C) excited at 647.1 nm. Conditions: same as in Figure 4.

Hb·$^{14}N_3$ excited at 638.3 nm. In addition, we observed at least two lines at 345 and 380 cm^{-1} (Figure 6A) which were not observed by Asher et al. (1977) in Fe(III)Hb·N_3. Comparison of Raman spectra of Fe(III)Mb·N_3 and Fe(III)Hb·N_3 excited at 647.1 nm (Figure 6A,C) reveals that these two lines are stronger in the myoglobin complex than in the hemoglobin complex. These additional modes in Fe(III)Mb·N_3 showed no change even when the ligand (azide) concentration was increased to >100 mM. We believed that these modes derive their intensities from high-spin species. Only the 411-cm^{-1} mode [in the case of Fe(III)Mb·N_3] exhibited a shift of 6 cm^{-1} to lower energy upon isotope substitution by $^{15}N_3$. Unlike the 573-cm^{-1} mode which was enhanced near or at the Soret band, the 411-cm^{-1} mode [or 414-cm^{-1} mode of Fe(III)Hb·N_3] is polarized. We therefore assign it to the Fe(III)–N_3 stretch, which is further supported by our normal coordinate analysis. As will be shown in our temperature-dependence studies, this Raman line derives its intensity from low-spin rather than high-spin species, which is contrary to the belief of Asher et al. (1977) although they did correctly assign the 413-cm^{-1} line in Fe(III)Hb·N_3 to Fe(III)–N_3 stretch.

The temperature dependence of the Raman spectrum of Fe(III)Mb·N_3 is displayed in Figure 7A (right panel), which demonstrates the intensity decrease of high-spin lines (1607 or 1544 cm^{-1}) relative to low-spin line (1642 cm^{-1}) upon a decrease in the temperature. The plot of the logarithm of the peak height intensity ratio, log (I_{1607}/I_{1642}), vs. $1/T$ is shown in the left panel of Figure 7A, from which the enthalpy change ($\Delta H°$) for the conversion of the low-spin to the high-spin state was estimated as ~2.9 kcal/mol. This value is only half the value obtained from infrared spectroscopy (5.6 kcal/mol) (Alben & Fager, 1972) but close to the one from magnetic susceptibility measurements (3.7 kcal/mol) (Iizuka & Kotani, 1969a). The plot of log (I_{1544}/I_{1642}) vs. $1/T$ is also included in Figure 7A. The smaller slope exhibited there may be caused by the overlapping low-spin porphyrin mode at 1541 cm^{-1}, as indicated in Figure 4C where Fe(III)Mb·Im is predominantly low spin.

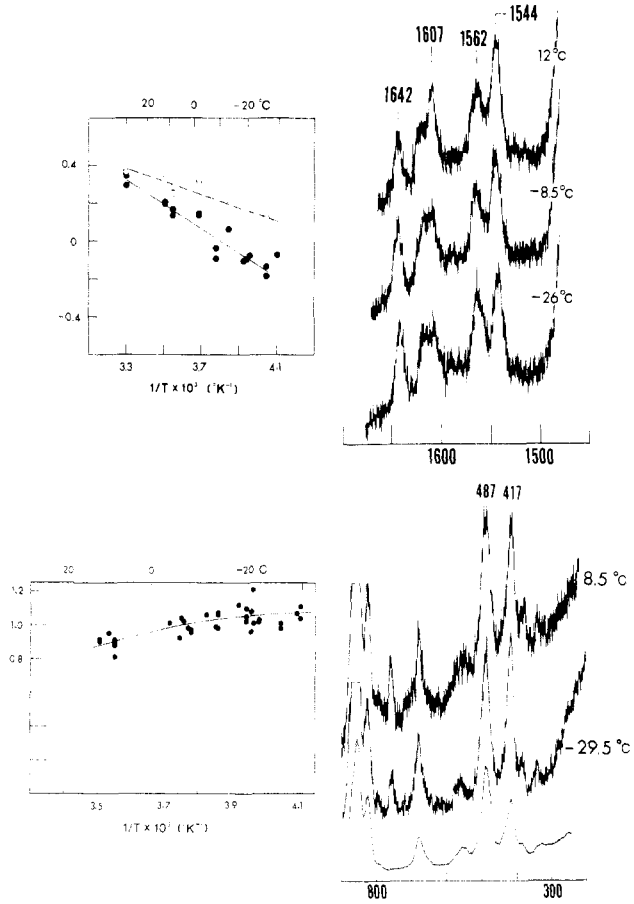

FIGURE 7: (A) Effect of temperature on the resonance Raman spectrum of metmyoglobin azide in the 1500–1700-cm^{-1} region. The logarithms of peak height intensity ratios, log (I_{1607}/I_{1642}) (●) and log (I_{1544}/I_{1642}) (○) are plotted against $1/T$. Conditions: λ, 647.1 nm; p, 375 mW at sample; slit width, 400 μm; scanning speed, 0.5 cm^{-1}/s; time constant, 5 s. Fe(III)Mb·N_3 (in 0.025 M sodium phosphate pH 7.2 buffer) was mixed with glycerol (final, 40% v/v) and then the pH value was adjusted to pH 7.2 at room temperature. Heme concentration, 0.66 mM; ligand concentrations 31 mM. (B) Effect of temperature on the resonance Raman spectrum of Fe(III)Mb·N_3 in the 300–800-cm^{-1} region. The intensity ratio of the 417-cm^{-1} line relative to the glycerol line at 487 cm^{-1} is plotted vs. $1/T$. Normal Raman spectrum of glycerol (in 0.025 M sodium phosphate pH 7.2 buffer) is shown for comparison in the bottom of right half. Experimental conditions are the same as described in (A).

Glycerol, which was employed as a cryosolvent, gives rise to two nonresonance Raman signals at 487 and 417 cm^{-1}, with the latter overlapping the Fe(III)–N_3 stretching mode at 411 cm^{-1}. As shown in Figure 7B, the 411-cm^{-1} intensity is about one-half of the observed intensity at 417 cm^{-1}. It was rather interesting to observe that the 417-cm^{-1} intensity (relative to the solvent at 487-cm^{-1} peak) shows a systematic increase with decreasing temperature (Figure 7B). This is *not* expected if the 411-cm^{-1} mode were due to high-spin species because the 640-nm band, characteristic of high-spin species, decreases with decreasing temperature. It is therefore a strong evidence that the 411-cm^{-1} mode in Fe(III)Mb·N_3 (or 414 cm^{-1} in Fe(III)Hb·N_3) may be enhanced via the weak low-spin, out of plant charge-transfer band at ~650 nm, rather than the stronger high-spin charge-transfer band at ~640 nm. Our normal coordinate calculations on isotope shifts confirm that it is indeed the Fe(III)–N_3 stretching vibration. At present, we have not observed any Raman line assignable to high-spin Fe(III)–N_3 stretch, nor had Yu & Tsubaki (1980) identified high-spin Mn(III)–N_3 stretch in their resonance Raman studies of Mn(III)Mb·N_3. We also have carried out similar temperature-dependence studies on Fe(III)Hb·N_3, but the effect of intensity increase at 417 cm^{-1} with decreasing temperature is less pronounced because of the predominant low-spin population (~95%) in hemoglobin complex compared to ~89% in myoglobin complex (Alben & Fager, 1972).

Low-spin modes at 1644 and 411 cm^{-1} in Fe(III)Mb·N_3 were strongly enhanced with excitation at 676.4 nm (not shown). On the other hand, the high-spin modes at 1607, 1544, 380, and 345 cm^{-1} are relatively weak. The stronger 411-cm^{-1} line relative to 380- and 345-cm^{-1} lines at 676.4-nm excitation than at 647.1 nm suggests that the low-spin charge-transfer band lies closer to the excitation wavelength at 676.4 nm than the high-spin charge-transfer band.

To provide a theoretical basis for our assignments, we have carried out a normal coordinate analysis on the model, azide–Fe–imidazole. The porphyrin was neglected in this model because it is assumed to be perpendicular to the plane containing the fifth and sixth ligands of iron, i.e., imidazole and azide, respectively. Imidazole was treated as a single dynamical unit with a mass of 68 amu. The structural parameters used are r(Fe–Im) = 2.00 Å, r(Fe–N_{azide}) = 2.10 Å, r(N=N) = 1.16 Å, ϕ(Im–Fe–N) = 180.0°, ϕ(Fe–N=N) = 112.6°, and ϕ(N=N=N) = 180.0°; these are based on the results of X-ray crystallographic studies on Fe(III)Mb·N_3, Fe(III)Hb·N_3, and several metal–azide complexes (Stryer et al., 1964; Deatherage et al., 1979; Jones, 1973). The Urey–Bradley force field was used for potential function, and the force constants were transferred from similar systems with slight adjustment for best fit. These force constants (in mdyn/Å) are $K(N_1{=}N_2) = K(N_2{=}N_3)$ = 12.93, K(Fe–N_3) = 1.20, K(Fe–Im) = 1.33, H(Fe–$N_3{=}N_2$) = 0.50, $H(N_1{=}N_2{=}N_3)_{\text{in plane}}$ = 0.60, $H(N_1{=}N_2{=}N_3)_{\text{out of plane}}$ = 0.60, H(N_3–Fe–Im)$_{\text{in plane}}$ = 0.57, and H(N_3–Fe–Im)$_{\text{out of plane}}$ = 0.57. Stretching–stretching interaction force constants between two adjacent bonds were F[(N=N) – (N=N)] = 1.74 mdyn/Å, F[(Fe–N) – (N=N)] = 0.44 mdyn/Å and F[(Fe–Im) – (Fe–N)] = 0.10 mdyn/Å. Deformation–deformation interactions between two angles were omitted in the calculation. The normal mode calculations were performed according to Wilson's GF matrix method (Wilson et al., 1955). The vibrational problem was defined in terms of the following internal coordinates: $R_1 = \nu(N_1{=}N_2)$, $R_2 = \nu(N_2{=}N_3)$, $R_3 = \nu$(Fe–N_3), $R_4 = \nu$(Fe–Im), $R_5 = \delta$(Fe–$N_3{=}N_2$), $R_6 = \delta_{\text{in plane}}(N_1{=}N_2{=}N_3)$, $R_7 = \delta_{\text{out of plane}}(N_1{=}N_2{=}N_3)$, $R_8 = \delta_{\text{in plane}}$($N_3$–Fe–Im), and $R_9 = \delta_{\text{out of plane}}$($N_3$–Fe–Im). There are a total of nine normal vibrations in this structural model. Compared in Table I are the calculated and observed frequencies in low-spin azide complexes. This provides a satisfactory account of the observed isotope shifts at ν_1 = 2023 cm^{-1}, ν_4 = 573 cm^{-1}, and ν_5 = 411 cm^{-1}.

Discussion

The charge-transfer transitions in heme proteins may derive from the electronic promotions between porphyrin and metal (Zerner et al., 1966; Eaton & Hochstrasser, 1968), between metal and axial ligands (Wright et al., 1979; Eaton et al., 1978), or between axial ligands and porphyrin (Yu & Tsubaki, 1980). The excitation from the highest occupied porphyrin π orbitals (a_{1u}, a_{2u}) to the vacant d orbitals of the iron such as (d_{xz}, d_{yz}) is not expected to enhance either the Fe–ligand stretch or the internal ligand vibrations because these bonding (or antibonding) orbitals are not involved and thus the excited-state geometry is not significantly distorted. This is consistent with the studies of high-spin acid ferricytochrome c by Lanir et al. (1979), who observed no Fe–axial ligand stretch but only the depolarized ring modes at 764, 1555, and

Table I: Comparison of Calculated and Observed Frequencies in Low-Spin Azide Complexes

no.	Im-Fe-$^{14}N_3$, calcd (cm^{-1})	Fe(III)Mb·$^{14}N_3$, obsd (cm^{-1})	Im-Fe-$^{15}N_3$, calcd (cm^{-1})	Fe(III)Mb·$^{15}N_3$, obsd (cm^{-1})	isotope shift calcd (obsd) (cm^{-1})	assignment[a]
ν_1	2023	2024	1955	1958	68 (65)	N=N antisym. stretch
ν_2	1341		1296		45	N=N sym. stretch
ν_3	695		672		23	N=N=N in-plane[b] bend
ν_4	569	573	550	554	19 (19)	N=N=N out of plane bend
ν_5	413	411	405	405	8 (6)	ν(Fe-N), 77%; +ν(Fe-Im), 13%, +δ(N=N=N), 9%
ν_6	251		248		3	Fe-Im stretch
ν_7	189		186		3	N-Fe-Im in-plane bend
ν_8	189		186		3	N-Fe-Im out of plane bend
ν_9	173		169		4	δ(Fe-N-N) 30% + δ(N=N=N) 20% + ν(Fe-Im) 13%

[a] ν(A-B), stretching of bond A-B. δ(A-B-C), bending of bond angle A-B-C. [b] The plane is defined by Fe and N=N=N. In the absence of interaction both in-plane and out of plane azide bending vibrations are degenerate (at ~640 cm^{-1}). In hydrogen azide they appear at 522 (in plane) and 672 cm^{-1} (out of plane) (Jones, 1973). The calculation here indicates that unlike HN_3 the out of plane bend (569 cm^{-1}) is lower than the in-plane bend (695 cm^{-1}).

1623 cm^{-1} upon excitation at ~620 nm, a charge-transfer band classified as band I according to Eaton & Hochstrasser (1968). The high-spin charge-transfer band at ~640 nm (x,y-polarized) in metmyoglobin azide is likely of the similar porphyrin (π) → high-spin iron (d_{xz}, d_{yz}) transition. The promotion from porphyrin (π) to iron a_{1g} (d_{z^2}) is possible and was in fact proposed by Churg & Makinen (1978) in low-spin oxymyoglobin.

The charge-transfer transition from a nonbonding orbital of the azide to a d_{z^2} orbital of the iron would enhance the Fe–N_3 stretch but not the internal azide vibrations. Upon excitation at ~650 nm we have observed the resonance enhancement at 411 cm^{-1} in Fe(III)Mb·N_3 (or 414 cm^{-1} in Fe(III)Hb·N_3), which is assigned as the Fe–N_3 stretch of the low-spin species (see Results). Because of the lack of internal azide mode enhancement, we proposed that the z-polarized charge-transfer band at ~650 nm (Eaton & Hochstrasser, 1968) is of the azide (n) → low-spin iron (d_{z^2}) type or porphyrin (π) → iron d_{z^2} type.

When azide π electrons are involved in charge-transfer transitions, one would expect the enhancement of internal azide vibrations. If the iron d_{z^2} orbital is also involved, the Fe–N_3 stretch should be enhanced as well. Consistent with this expectation, upon Soret excitation both Fe–N_3 stretch[1] and nontotally symmetric azide modes (573 cm^{-1}, out of plane bending; 2024 cm^{-1}, antisymmetric stretch) from the low-spin component were detected. This is indicative of the existence of a low-spin charge-transfer transition near the Soret band, which may be assignable as azide (π) → low-spin iron (d_{z^2}). The resonance enhancement of nontotally symmetric azide modes requires that the proposed charge-transfer state is capable of mixing with the Soret state via Herzberg–Teller vibronic couplings (Yu & Tsubaki, 1980). It is of interest to note that these azide modes are not resonance enhanced in cytochrome c heme octapeptide azide complex with the same Soret excitation (R. B. Srivastava and N.-T. Yu, unpublished experiments), suggesting that the charge-transfer band may have been shifted away and that the Soret band alone is not sufficient to bring out the azide vibrations.

[1] The Fe(III)–N_3 stretch at 411 cm^{-1} in Fe(III)Mb·N_3 is accidentally degenerate with a much stronger ring mode at 411 cm^{-1} upon Soret excitation making it difficult to ascertain its existence. However, in the spectrum of Fe(III)Hb·N_3 the ring mode at 411 cm^{-1} is shifted to ~420 cm^{-1} with a much reduced intensity. We clearly observed the appearance of an isotope-sensitive mode at ~407 cm^{-1} when $^{14}N_3$ was replaced by $^{15}N_3$ (M. Tsubaki and N.-T. Yu, unpublished experiments).

Finally, the observation of antisymmetric stretch at ~2046 cm^{-1} from the high-spin species of Fe(III)Mb·N_3 suggests the existence of an additional charge-transfer transition near the Soret band. The nature of this transition is unknown, although it may be tentatively assigned as azide (π) → porphyrin (π^*) in analogy to a similar transition in Mn(III)Mb·N_3, where no Mn–N_3 stretch (or Fe–N_3 stretch) can be enhanced (Yu & Tsubaki, 1980).

References

Alben, J. O., & Fager, L. Y. (1972) *Biochemistry 11*, 842.

Asher, S. A., & Schuster, T. M. (1979) *Biochemistry 18*, 5377.

Asher, S. A., Vickery, L. E., Schuster, T. M., & Sauer, K. (1977) *Biochemistry 16*, 5849.

Beetlestone, J. G., & George, P. (1964) *Biochemistry 3*, 707.

Champion, P. M., Gunsalus, I. C., & Wagner, G. C. (1978) *J. Am. Chem. Soc. 100*, 3743.

Churg, A. K., & Makinen, M. W. (1978) *J. Chem. Phys. 68*, 1913.

Deatherage, J. F., Obendorf, S. K., & Moffat, K. (1979) *J. Mol. Biol. 134*, 419.

Desbois, A., Lutz, M., & Banerjee, R. (1979) *Biochemistry 18*, 1510.

Desbois, A., Lutz, M., & Perutz, M. F. (1980) *Proceedings of VIIth International Conference on Raman Spectroscopy* (Murphy, W. F., Ed.) pp 576–577, North-Holland Publishing Co., Amsterdam, New York.

Eaton, W. A., & Hochstrasser, R. M. (1968) *J. Chem. Phys. 49*, 985.

Eaton, W. A., Hanson, L. K., Stephens, P. J., Sutherland, J. C., & Dunn, J. B. R. (1978) *J. Am. Chem. Soc. 100*, 4991.

Iizuka, T., & Kotani, M. (1968) *Biochim. Biophys. Acta 154*, 417.

Iizuka, T., & Kotani, M. (1969a) *Biochim. Biophys. Acta 181*, 275.

Iizuka, T., & Kotani, M. (1969b) *Biochim. Biophys. Acta 194*, 351.

Iizuka, T., & Yonetani, T. (1970) *Adv. Biophys. 1*, 157.

Jones, K. (1973) in *Comprehsneive Inorganic Chemistry* (Trotman-Dickenson, A. F., Ed.) Vol. 2, Chapter 19, pp 276–293, Pergamon Press, Elmsford, NY.

Kilmartin, J. V., Hewitt, J. A., & Wooton, J. F. (1975) *J. Mol. Biol. 93*, 203.

Kitagawa, T., Kyogoku, Y., Iizuka, T., & Saito, M. I. (1976) *J. Am. Chem. Soc. 98*, 5169.

Lanir, A., Yu, N.-T., & Felton, R. H. (1979) *Biochemistry 18*, 1656.

McCoy, S., & Caughey, W. S. (1970) *Biochemistry 9*, 2387.
Spaulding, L. D., Chang, R. C. C., Yu, N.-T., & Felton, R. H. (1975) *J. Am. Chem. Soc. 97*, 2517.
Spiro, T. G. & Strekas, T. C. (1974) *J. Am. Chem. Soc. 96*, 338.
Spiro, T. G., Stong, J. D., & Stein, P. (1979) *J. Am. Chem. Soc. 101*, 2648.
Stryer, L., Kendrew, J. C., & Watson, H. C. (1964) *J. Mol. Biol. 8*, 96.
Wilson, E. B., Jr., Decius, J. C., & Cross, P. C. (1955) *Molecular Vibrations*, McGraw-Hill, New York.
Wright, P. G., Stein, P., Burke, J. M., & Spiro, T. G. (1979) *J. Am. Chem. Soc. 101*, 3531.
Yu, N.-T., & Srivastava, R. B. (1980) *J. Raman Spectrosc. 9*, 166.
Yu, N.-T., & Tsubaki, M. (1980) *Biochemistry 19*, 4647.
Zerner, M., Gouterman, M., & Kobayashi, H. (1966) *Theor. Chim. Acta 6*, 363.

Insights into Heme Structure from Soret Excitation Raman Spectroscopy†

Patricia M. Callahan and Gerald T. Babcock*

ABSTRACT: Laser lines in resonance with the Soret band optical transitions of several heme proteins and heme model compounds have been used to obtain Raman spectra of these species. Correlations between the observed frequency of a polarized mode in the 1560–1600-cm^{-1} region and the heme iron spin and coordination geometry have been developed. The position of this band is also a function of the pattern of porphyrin pyrrole ring β-carbon substitution, and therefore structural information can be extracted from the Raman data only after this dependence has been taken into account. Quantitative correlations between the frequency of this band and the porphyrin core size are presented for three commonly occurring classes of heme compounds: (a) protoheme derivatives, (b) iron porphyrins in which all ring positions are saturated, and (c) heme *a* species. A polarized mode in the 1470–1510-cm^{-1} region is also consistently enhanced upon Soret excitation of these compounds, but is relatively insensitive to peripheral substituents, and can be used in conjunction with the polarized mode described above to assign heme geometries. In the frequency region above 1600 cm^{-1}, a vibration is observed which also responds to changes in porphyrin geometry. However, this band is sometimes obscured by vibrations of unsaturated β-carbon substituents, particularly in the case of protoheme derivatives. The normal coordinate analysis developed by Abe and co-workers [Abe, M., Kitagawa, T., & Kyogoku, Y. (1978) *J. Chem. Phys. 69*, 4526–4534] is used to rationalize the dependence of the various modes on porphyrin geometry and peripheral substitution.

The geometry of the porphyrin macrocycle in hemes and heme proteins is reflected in the frequency positions of several vibrational bands observed by resonance Raman spectroscopy (Spiro, 1974; Felton & Yu, 1978; Kitagawa et al., 1978; Rousseau et al., 1979). One of the most useful empirical correlations between heme structure and Raman frequency has been developed by Spaulding et al. (1975), who showed that an inverse relationship exists between the frequency of an anomalously polarized mode in the 1550–1610-cm^{-1} region and C_t–N, the distance from the center of the porphyrin to the pyrrole nitrogens. This was later confirmed and extended (Huong & Pommier, 1977; Scholler & Hoffman, 1979; Spiro et al., 1979), and plots of Raman frequency vs. porphyrin core size (C_t–N) for the ap[1] mode (denoted band IV) as well as for a polarized mode in the 1470–1510-cm^{-1} region (band II) and for a depolarized mode in the 1600–1650-cm^{-1} region (band V) could be fit by an empirical equation of the form

$$\bar{\nu}_i = K_i(A_i - d) \text{ cm}^{-1} \quad (1)$$

where $\bar{\nu}_i$ is the frequency of the vibration under consideration, d the C_t–N distance, and K_i and A_i are adjustable parameters specific to the ith vibration. Equation 1 has thus far been established for the three vibrational bands indicated above, all of which have appreciable methine bridge bond stretching character (Spiro et al., 1979). As a consequence, the correlations indicated by eq 1 are relatively insensitive to the nature of the pyrrole β-carbon substituents, provided that these are linked by C_β–C_s bonds. However, replacement of the hydrogen at the methine bridge carbon by, for example, phenyl groups or deuterium, causes shifts in these bands unrelated to core size change, and eq 1 is no longer applicable. In addition, bands II and V are also somewhat sensitive to the nature of the axial ligands and shift to higher frequency as the π acceptor character of the ligands is increased.

With the establishment of sound correlations between porphyrin core size and Raman frequency, it has become possible to interpret scattering data to determine both spin state and iron coordination number for several heme proteins (Spiro et al., 1979; Sievers et al., 1979). However, the research which has been done thus far to link porphyrin core size and Raman vibrational frequencies has been carried out with α,β excitation. Under these conditions Herzberg–Teller scattering dominates, and, for a porphyrin of D_{4h} symmetry, enhancement of modes of A_{2g}, B_{1g}, and B_{2g} symmetry is strong whereas A_{1g} modes are weak or absent (Friedman & Hochstrasser, 1973; Felton & Yu, 1978; Rousseau et al., 1979). For Soret excitation, on the other hand, scattering occurs by a Franck–Condon mechanism, and the opposite pattern of vibrational enhancement is observed: polarized modes dominate the spectrum, and anomalously polarized and depolarized lines are weak. Additionally, depolarized modes can acquire A-term intensity

† From the Department of Chemistry, Michigan State University, East Lansing, Michigan 48824. *Received July 16, 1980.* This investigation was supported by National Institutes of Health Grant No. GM25480.

[1] Abbreviations used: ap, anomalously polarized; Me_2SO, dimethyl sulfoxide; dp, depolarized; Hepes, *N*-(2-hydroxyethyl)piperazine-*N*′-2-ethanesulfonic acid; HRP, horseradish peroxidase; NMeIm, *N*-methylimidazole; OEP, octaethylporphyrin; p, polarized; PPIX DME, protoporphyrin IX dimethyl ester; $NaDodSO_4$, sodium dodecyl sulfate.

0006-2960/81/0420-0952$01.00/0